Matching Rules for Collective Behaviors on Complex Networks: Optimal Configurations for Vibration Frequencies of Networked Harmonic Oscillators

Meng Zhan[1]*, Shuai Liu[1,2], Zhiwei He[1,2]

1 Wuhan Center for Magnetic Resonance, State Key Laboratory of Magnetic Resonance and Atomic and Molecular Physics, Wuhan Institute of Physics and Mathematics, Chinese Academy of Sciences, Wuhan, China, **2** University of the Chinese Academy of Sciences, Beijing, China

Abstract

The structure-dynamics-function has become one of central problems in modern sciences, and it is a great challenge to unveil the organization rules for different dynamical processes on networks. In this work, we study the vibration spectra of the classical mass spring model with different masses on complex networks, and pay our attention to how the mass spatial configuration influences the second-smallest vibrational frequency (ω_2) and the largest one (ω_N). For random networks, we find that ω_2 becomes maximal and ω_N becomes minimal if the node degrees are point-to-point-positively correlated with the masses. In these cases, we call it point-to-point matching. Moreover, ω_2 becomes minimal under the condition that the heaviest mass is placed on the lowest-degree vertex, and ω_N is maximal as long as the lightest mass is placed on the highest-degree vertex, and in both cases all other masses can be arbitrarily settled. Correspondingly, we call it single-point matching. These findings indicate that the matchings between the node dynamics (parameter) and the node position rule the global systems dynamics, and sometimes only one node is enough to control the collective behaviors of the whole system. Therefore, the matching rules might be the common organization rules for collective behaviors on networks.

Introduction

Various dynamical processes on complex networks [1–16] have attracted a great deal of interest in many disciplines, ranging from physical, chemical, and biological sciences, to even social sciences and engineering technology, with the central target to decipher and even utilize the emergent features coming out of the interplay between the structure and function via dynamics. Since a function is a dynamic property, the structure-dynamics-function has been one of common problems in modern sciences [1–5]. These dynamical behaviors can be very rich including synchronization in coupled nonlinear systems, consensus or grouping in multi-agent systems, self-organized criticality, epidemic spreading, traffic jam, stochastic resonance, and many others. They pose astonishing challenges for us to unveil the organization rules for all these different dynamical processes on networks.

So far the dynamics on extensive systems composed of many coupled identical units has been extensively studied, for example, the complete synchronization in coupled chaotic systems based on the stability analysis of the synchronous manifold and in the framework of the master stability function [17–23]. However, the assumption of identical units is not very realistic for many realistic systems, in which the units composing the ensemble always present a disparity in the values of some characteristic parameters. Under these conditions, the system (parameter) diversity becomes very important [24–29]. It is, however, still unknown how these nodes with different characteristic parameters settled on networks determine the systems dynamics, especially when some key parameters are properly placed on some special positions of networks. This optimal configuration problem has never been carefully studied, to the best knowledge of the authors, although it certainly could help to better understand the collective behaviors of coupled nonidentical systems, which are determined by not only the interplay between the temporal information (the node dynamics with different parameters) and the spatial information (these nodes' positions on networks), but also their matchings.

For this purpose, we study the optimal configuration problem for the vibration spectrum (or frequencies) of coupled nonidentical harmonic oscillators on complex networks. Each vertex is occupied by a mass point and they are connected by an edge (spring) each other with a uniform spring constant. This mass-spring (linear) model and the normal mode analysis originally developed in classical mechanics [30,31], have been found very useful in many other disciplines, such as lattice vibrations and associated phonon excitations in solid-state physics [32], and protein dynamics in structural biology [33,34]. As we are interested in the diversity effect, we only consider the case for each node having a different mass; this is the key distinction with all previous studies on coupled harmonic oscillators [35–38].

Model and Results

Model

The motion equation for the systems can be written as

$$m_j \ddot{x}_j = \kappa \sum_{i=1}^{N} a_{ij}(x_i - x_j), \quad j = 1, \cdots, N \qquad (1)$$

where m_j represents the j-th oscillator's mass, κ is the coupling strength (or spring coefficient), and N represents the number of mass points. $a_{ij} = 1$ if nodes i and j are connected and $a_{ij} = 0$ otherwise. For simplicity, we take $\kappa \equiv 1$ throughout the paper. The masses m_j for all j are different. The system's motion can be viewed as N normal modes with different frequencies: $x_j = \sum_{i=1}^{N} y_j e^{i\omega_i t}$, where ω_i and y_j denote one independent frequency and the amplitude, respectively. $\omega_1 \leq \omega_2 \leq \ldots \leq \omega_N$. Clearly $\omega_1 = 0$, representing the translational motion. For the other modes, usually the second smallest (slowest) vibration frequency ω_2 characterizes the most global vibrational motion of the systems, whereas the largest vibration frequency ω_N reflects the most tightly packed and constrained local motion; both of them are the most representative. Therefore, below we only consider the values of ω_2 and ω_N for different spatial configurations of the masses.

The above equations [Eqs. (1)] can be written in a compact form based on the normal mode analysis:

$$(\omega^2 M - L)Y = 0, \qquad (2)$$

where the mass matrix $M = diag(\{m_j\})$, the Laplacian matrix $L = (\delta_{ij} d_i - a_{ij})$, where $\delta_{ij} = 1$ for $i = j$ and $\delta_{ij} = 0$ otherwise, d_i is the degree of node i, and Y is the N-dimensional nonzero column vector with the components y_i.

Solving Eqs. (2) is equivalent to finding ω satisfying $\det(\omega^2 M - L) = 0$, where "det" denotes the determinant. Since M is nonsingular, it is convenient to change the mass-weighted Laplacian matrix to a symmetric one and get a faster numerical result. Therefore, we have

$$\omega^2 = \lambda(M^{-1}L) = \lambda(M^{-1/2}LM^{-1/2}), \qquad (3)$$

where λ denotes the eigenvalue of the corresponding matrix. And we obtain ω based on solving the eigenvalues of the symmetrical matrix $M^{-1/2}LM^{-1/2}$ for a given network. In numerics, we have studied various networks, such as the random Erdos-Renyi (ER) [39], scale-free (SF) [40], and small-world (SW) [41] networks. For each network, an ensemble of masses is produced from a random distribution ($1 \leq m_j \leq 10$) and these values are fixed and scattered on networks. For each configuration, its vibration frequencies can be easily calculated from the above eigenvalue analysis [Eq. (3)]. We are interested in how the correlation between degrees and masses influences the normal mode frequencies ω_2 and ω_N.

Simulation results

Figure 1(a) illustrates the numerical results of ω_2 in an ascending order for completely random configurations (i.e., all masses can be arbitrarily shuffled on complex networks); a random ER network ($N = 200$ and the average degree $\langle d \rangle = 30$) is chosen here. The corresponding distribution re-scaled by the peak value is given in Fig. 1(b). Clearly ω_2 shows a very wide distribution from $\omega_2 \approx 1.2$ to $\omega_2 \approx 1.65$. However, we may also choose configurations purposefully, such as point-to-point-positive correlation between

the node masses and the node degrees (namely, we may arrange the masses in an ascend order $\{m_1 \leq m_2 \leq \ldots \leq m_N\}$ and the degrees in an ascend order also $\{d_1 \leq d_2 \leq \ldots \leq d_N\}$, and put these arranged masses on the network in a point-to-point-positive correlation order $\{d_1/m_1, d_2/m_2, \ldots, d_N/m_N\}$). We really find its ω_2 for this configuration is maximal, as shown the open square in Figs. 1(a) and 1(b). Correspondingly, for the configuration of point-to-point-negative correlation $\{d_1/m_N, d_2/m_{N-1}, \ldots, d_N/m_1\}$ illustrated by a solid square, it seems that ω_2 is very small.

Below let us see if the above strong correlation condition for the point-to-point matching could be loosened. Figure 1(c) shows the results for the single-point-positive correlation $\{d_1/m_1\}$ (upper curve) and $\{d_N/m_N\}$ (lower curve), with all other $N - 1$ masses randomly placed. Here we use $\{d_1/m_1\}$ to denote the configuration of putting the lightest mass on the lowest-degree node, whereas $\{d_N/m_N\}$ for that of the heaviest on the highest-degree node. It is discernible that the curve for $\{d_1/m_1\}$ is slightly above the counterpart for $\{d_N/m_N\}$, which is quite similar to that for the random configurations in 1(a). Moreover, Figs. 1(d) and 1(e) show the results for the single-point-negative correlation $\{d_N/m_1\}$ and $\{d_1/m_N\}$, respectively, with all other $N - 1$ masses randomly placed again. Clearly the distribution in 1(d) is still similar to that for the random configurations in 1(a). However, very remarkably
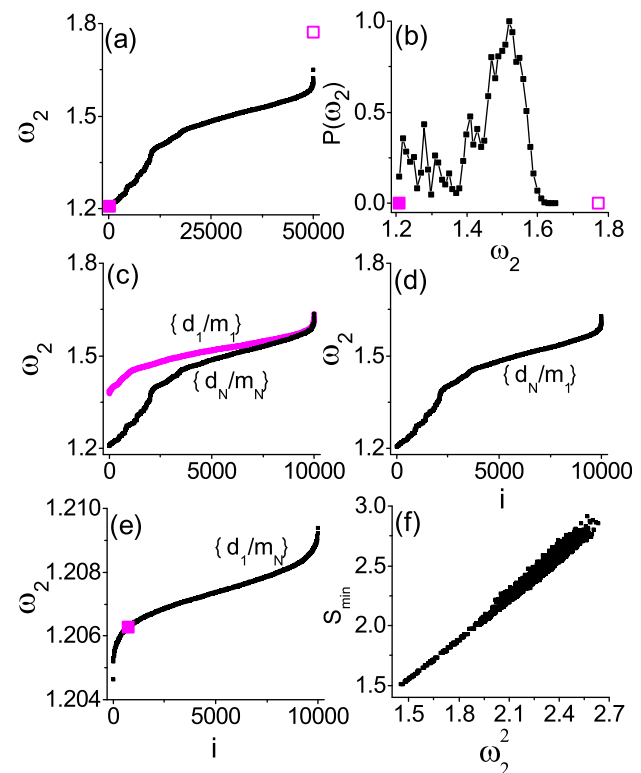

Figure 1. The results of ω_2 for a random ER network. $N = 200$, $\langle d \rangle = 30$, $d_{\min} = 15$, and $d_{\max} = 41$, the plot includes completely random configurations (black points), the point-to-point-positive correlation configuration (open squares), and the point-to-point-negative correlation configuration (solid squares) in (a); the single-point-positive correlation configurations $\{d_1/m_1\}$ and $\{d_N/m_N\}$ in (c); and the single-point-negative correlation configurations $\{d_N/m_1\}$ in (d) and $\{d_1/m_N\}$ in (e). (b) The histogram for random configurations. (f) $S_{\min}$ vs ω_2^2. A remarkable finding in (e) is ω_2's are not only very small, but also their range is very narrow, indicating one is enough in determining the networked dynamics. For more details, see the text.
doi:10.1371/journal.pone.0082161.g001

the values of ω_2 for $\{d_1/m_N\}$ (with one and only one heaviest mass on the lowest degree) have been greatly squeezed into a much smaller regime: $1.204 < \omega_2 < 1.210$ and they are indeed very small [noticing the different ordinates and their scales used in Figs. 1(a) and 1(e)]. This range is only one-hundredth of the original range for the random distribution or other single-point matching distributions. We also find that ω_2 for the point-to-point-negative correlation in Fig. 1(a) is not minimal, which is re-plotted in Fig. 1(e) with the same solid square. This indicates that the single-point matching $\{d_1/m_N\}$ has already caught the essential feature of the collective behavior in such a model of harmonic oscillators on random networks, regardless of all other nodes. As a result, for ω_2, the single-point matching $\{d_1/m_N\}$ should give rise to $(\omega_2)_{\min}$, whereas the point-to-point matching $\{d_1/m_1, d_2/m_2, \ldots, d_N/m_N\}$ should lead to $(\omega_2)_{\max}$, although these observations still need proof in theoretical analysis.

Figure 2 presents the results for ω_N instead with the same random network and the ensemble of masses. For the random configurations, ω_N's are distributed in a very wide range $(5.0 < \omega_N < 6.2)$. The configurations for the point-to-point-positive correlation and the point-to-point-negative correlation, as shown the open and solid squares in Fig. 2(a), give rise to the minimal and maximal values of ω_N, respectively. They are just opposite to those for ω_2. Again ω_N for the configuration of point-to-point-positive correlation is very far from the distribution in 2(b). In Figs. 2(c) and 2(e), the single-point matching distributions for $\{d_1/m_1\}$, $\{d_N/m_N\}$, and $\{d_1/m_N\}$ give no significant difference with that for the random distribution. However, for the single-point-negative correlation $\{d_N/m_1\}$ in 2(d), we do find ω_N's have been squeezed into a much smaller regime; this time it corresponds to the part of the largest ω_N. All these findings show the key qualitatively unchanged features with those for ω_2.

To show the generality of matching rules for any random networks, we give some more examples. For instance, the results for a scale-free network ($\mathcal{N} = 200$ and $\langle d \rangle = 50$) with a randomly distributed ensemble of masses are shown in Figs. 3(a)–3(h). Figure 3(a) illustrates ω_2 for random configurations with the two extreme points (open and solid squares) for the configurations (point-to-point-positive and point-to-point-negative correlations). The histogram is shown in 3(b). Again Fig. 3(c) exhibits the unusual effect of single-point-negative correlation $\{d_1/m_N\}$ for ω_2, indicative of an insensitivity of vibration frequency if the temporal information and spatial information of only one node are matched. Similarly, Figs. 3(e)–3(h) give the patterns for ω_N, showing the same qualitative results as in Fig. 2.

Figures 4(a)–4(d) illustrate the distributions of ω_2 for random configurations of a SW network with some different rewiring probabilities P: $P = 0.4, 0.3, 0.2$, and 0.1, respectively; $\mathcal{N} = 200$ and $\langle k \rangle = 30$. The open and solid squares represent the configurations of point-to-point-positive and point-to-point-negative correlations between the node masses and node degrees, respectively. Clearly with increasing random connections for larger P, such as the plots in Figs. 4(a) and 4(b), the two points keep as extreme, locating far away the distribution for random configurations. However, with decreasing random connections for smaller P, as shown in 4(c) and 4(d), these relations become broken. Based on these comparisons, we understand that the rules of point-to-point matching and the single-point matching may only work for sufficiently random networks, such as ER or SF networks, and these rules could gradually be broken with the weakening of the network random connections, such as the SW networks.
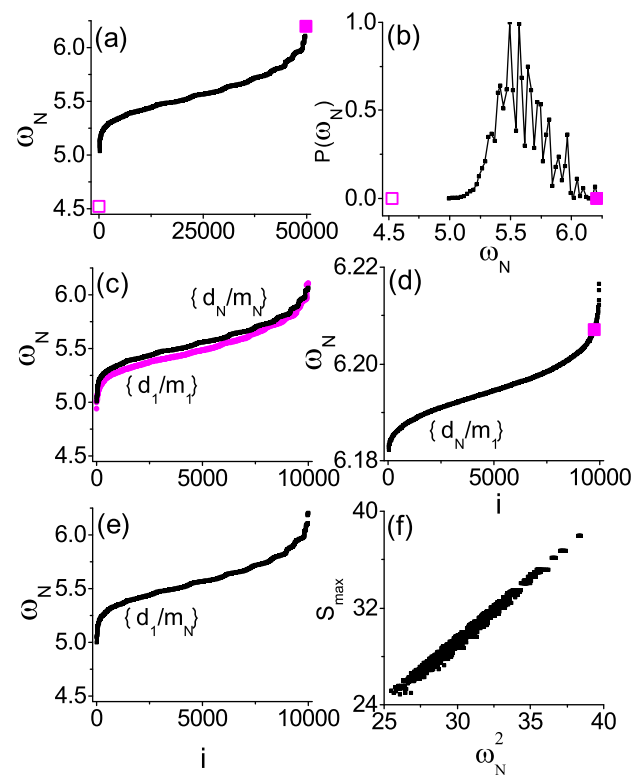

Figure 2. The results of ω_N for a random ER network. Similar to Fig. 1 for the results of ω_N with the same ER network considered instead. Again the effect of one is enough appears, but this time ω_N becomes maximal for the single-point-negative correlation configuration $\{d_N/m_1\}$ in (d). For more details, see the text.
doi:10.1371/journal.pone.0082161.g002

Analysis

So far some unusual effects of matching rules have been well revealed. Below let us demonstrate them in a rigid way with the aid of mathematical analysis. As we have known, the normal mode frequencies are solely determined by the mass-weighted Laplacian matrix [Eq. (3)]. Therefore, some approximation results for the weighted Laplacian matrix developed in the matrix algebra and applied in the chaos synchronization study should be very valuable for our problems here [20,21,42]; for the second smallest and largest eigenvalues λ_2 and λ_N, we have

$$S_{\min}\mu_2 c \le \lambda_2 \le S_{\min}c', \quad S_{\max} \le \lambda_N \le S_{\max}\mu_N, \qquad (4)$$

where c and c' can be approximated by 1 for most complex networks, and S_i, the intensity function of a node, is defined as $S_i = \sum_{j=1}^{N} W_{ij}a_{ij}$, where W_{ij} is the element of the weighted matrix. Since $W_{ij} = 1/m_i$ here, we have $S_i = \frac{d_i}{m_i}$ and further

$$S_{\min} = \min\{\frac{d_i}{m_i}, i = 1, \cdots, N\},$$
$$S_{\max} = \max\{\frac{d_i}{m_i}, i = 1, \cdots, N\}. \qquad (5)$$

When the network is sufficiently random ($d_{\min} \gg 1$ and $d_{\min} \gg \sqrt{\langle d \rangle}$),

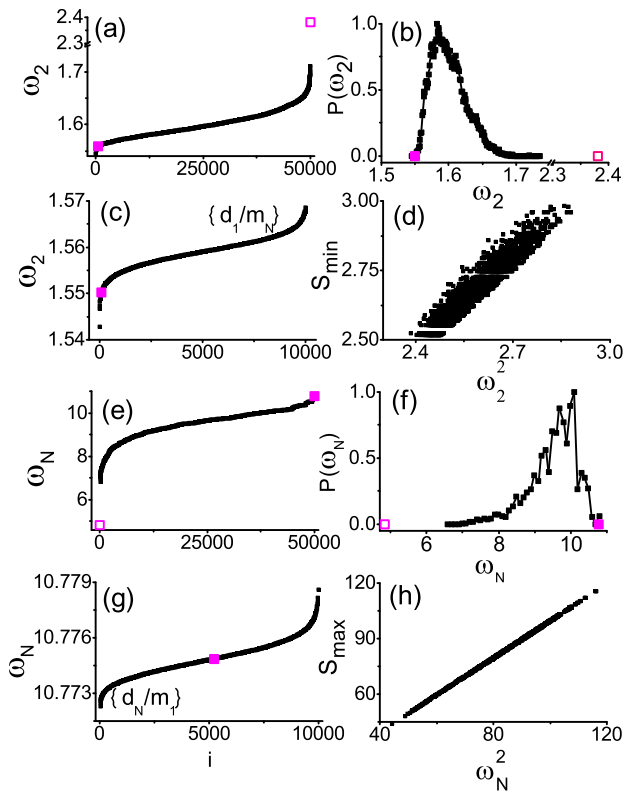**Figure 3. The results of ω_2 and ω_N for a scale-free network.** Similar to Figs. 1 and 2 for a scale-free network ($N = 200$, $\langle d \rangle = 50$, $d_{\min} = 25$, and $d_{\max} = 125$) instead.
doi:10.1371/journal.pone.0082161.g003

Figure 4. Histograms of ω_2 for random configurations of a SW network. (a)–(d) $N = 200$ and $\langle k \rangle = 30$ with different rewiring probabilities P: $P = 0.4$, 0.3, 0.2, and 0.1, respectively. The open and solid squares represent the configurations of point-to-point-positive and point-to-point-negative correlations between the node masses and node degrees, respectively.
doi:10.1371/journal.pone.0082161.g004

$$\mu_2 \simeq 1 - \frac{2}{\sqrt{\langle d \rangle}}, \quad \mu_N \simeq 1 + \frac{2}{\sqrt{\langle d \rangle}}. \qquad (6)$$

Therefore, for a sufficiently large $\langle d \rangle$,

$$\lambda_2 \simeq S_{\min}, \lambda_N \simeq S_{\max}. \qquad (7)$$

As a result, λ_2 and λ_N (and hence ω_2 and ω_N correspondingly) should be completely determined by $S_{\min}$ and $S_{\max}$, respectively.

These linear relations have been perfectly proved by our simulations, for example, the plot of $S_{\min}$ versus ω_2^2 in Fig. 1(f) and that of $S_{\max}$ versus ω_N^2 in 2(f). Based on these analyses [Eq. (5)], we immediately know that the configuration of single-point-negative correlation $\{d_1/m_N\}$ (with the heaviest mass on the lowest-degree node) should always give rise to $(S_{\min})_{\min}$ and $(\omega_2)_{\min}$ irrespective of all other masses. Here one node match is dominant.

The result for point-to-point-positive correlation for $(\omega_2)_{\max}$ can also be easily understood. Without losing generality, suppose that the masses and the degrees have been perfectly placed, i.e.,

$$\{\frac{d_1}{m_1}, \ldots, \frac{d_u}{m_u}, \ldots, \frac{d_v}{m_v}, \ldots, \frac{d_N}{m_N}\}. \qquad (8)$$

Here $u < v$, $d_u \leq d_v$ and $m_u \leq m_v$. If any one pair of nodes (u-th and v-th) are not placed in order, namely, node with mass m_u is placed on the node of degree d_v while m_v on d_u instead, we have the new configuration
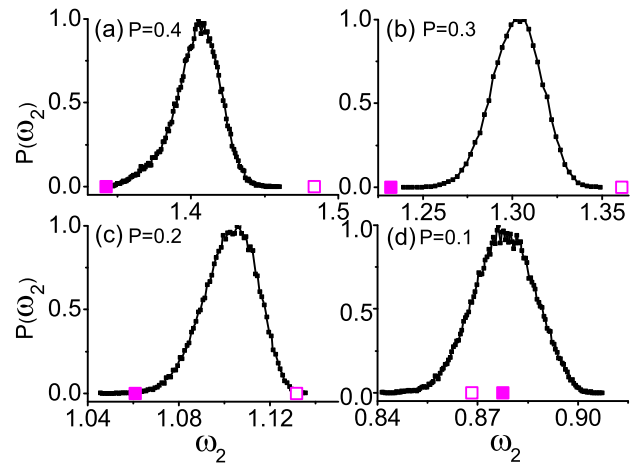
$$\{\frac{d_1}{m_1}, \ldots, \frac{d_u}{m_v}, \ldots, \frac{d_v}{m_u}, \ldots, \frac{d_N}{m_N}\}. \qquad (9)$$

Based on the following inequalities

$$\frac{d_u}{m_v} \leq \frac{d_v}{m_u}, \quad \frac{d_u}{m_v} \leq \frac{d_u}{m_u}, \quad \frac{d_u}{m_v} \leq \frac{d_v}{m_v}, \qquad (10)$$

giving rise to

$$\min\{\frac{d_u}{m_v}, \frac{d_v}{m_u}\} = \frac{d_u}{m_v} \leq \min\{\frac{d_u}{m_u}, \frac{d_v}{m_v}\}, \qquad (11)$$

we can derive that any one permutation from the original, perfect configuration of the point-to-point-positive correlation [Eq. (8)] would not let $S_{\min}$ increase. Therefore, the original configuration would be globally optimal, corresponding to $(\omega_2)_{\max}$. On the other hand, we may use the same idea to the analysis of $S_{\max}$ for $(\omega_N)_{\min}$.

Finally after mastering these features of coupled harmonic oscillators, we may even control the systems collective behavior by a slight manipulation [43–45]. E.g., a single node with the heaviest mass $m = 10$ ($1 \leq m_j \leq 10$) has been added and connected to any nodes of an ER network, as shown in Fig. 5, where the lower part represents $\mathcal{N}$ trials with one connection and the higher part represents $\mathcal{Z}$ ($Z = C_N^2 = N(N-1)/2$) trials with any two connections; $\mathcal{N} = 200$. Therefore, we have $\omega_2 \approx \sqrt{1/10} \approx 0.32$ for the lower value and $\omega_2 \approx \sqrt{2/10} \approx 0.45$ for the higher value. In contrast, the original big value $\omega_2 = 1.48$ is illustrated by a dashed line. By this method, we may accomplish precise control of ω_2. Similar results have also been obtained for other networks.

Discussion

In conclusion, we have studied the parameter diversity effect of coupled harmonic oscillators with different masses on complex networks, and found that the values of ω_2 and ω_N highly depend
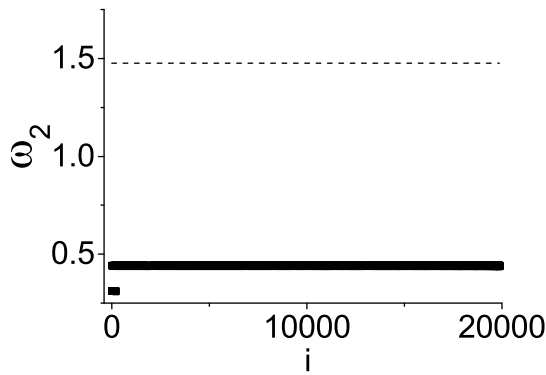
Figure 5. Controllability of network. Control of ω_2 by adding one node ($m = 10$) and connecting it to any one node (lower part) and any two nodes (higher part) in an ER network, the same as in Figs. 1 and 2, in contrast to the uncontrolled value of ω_2 (dashed line).
doi:10.1371/journal.pone.0082161.g005

on the configurations of these masses on the network spatial structure. Especially, two key matching rules including the point-to-point matching and single-point matching determine their extreme values. These findings might be helpful for explaining

some interesting phenomena, such as biological swarming and flocking in nature, where the match of the head's ability with its position in hierarchy is always crucial for the behaviors of the whole group. In addition, the optimal configuration not only exhibits the importance of matching between the node dynamics and the node position and their impact on the collective behaviors of coupled systems, but also provides a potential control method for the manipulation of the systems dynamics. A possible candidate for this might be the point mutation in the protein dynamics study. We expect that the feature of "one is enough" may arouse general interest in studying the structure-dynamics-function relation in complex systems, and the matching rules may also become the common organization rules for various dynamical processes on complex networks.

Acknowledgments

Author Contributions

Conceived and designed the experiments: MZ. Performed the experiments: MZ SL ZH. Analyzed the data: SL MZ ZH. Contributed reagents/materials/analysis tools: SL MZ ZH. Wrote the paper: MZ SL.

References

1. Bar-Yam Y (1997) Dynamics of Complex Systems. Westview Press.
2. Newman MEJ (2009) Networks: an introduction. Oxford University Press.
3. Rigoutsos I, Stephanopoulos G (2006) Systems Biology: Volume II: Networks, Models, and Applications. Oxford University Press, USA.
4. Serdyuk IN (2007) Methods in molecular biophysics: structure, dynamics, function. Cambridge University Press.
5. Trappenberg TP (2010) Fundamentals of computational neuroscience. Oxford University Press.
6. Boccaletti S (2008) The Synchronized Dynamics of Complex Systems. Elsevier Science.
7. Boccaletti S, Grebogi C, Lai YC, Mancini H, Maza D (2000) The control of chaos: theory and applications. Physics reports 329: 103–197.
8. Boccaletti S, Kurths J, Osipov G, Valladares D, Zhou C (2002) The synchronization of chaotic systems. Physics Reports 366: 1–101.
9. Albert R, Barabási AL (2002) Statistical mechanics of complex networks. Reviews of modern physics 74: 47–97.
10. Arenas A, Díaz-Guilera A, Kurths J, Moreno Y, Zhou C (2008) Synchronization in complex networks. Physics Reports 469: 93–153.
11. Dorogovtsev SN, Goltsev AV, Mendes JF (2008) Critical phenomena in complex networks. Reviews of Modern Physics 80: 1275–1335.
12. Zou W, Wang XG, Zhao Q, Zhan M (2009) Oscillation death in coupled oscillators. Frontiers of Physics in China 4: 97–110.
13. Zou W, Zheng X, Zhan M (2011) Insensitive dependence of delay-induced oscillation death on complex networks. Chaos: An Interdisciplinary Journal of Nonlinear Science 21: 023130–023130.
14. Woodman MM, Jirsa VK (2013) Emergent dynamics from spiking neuron networks through symmetry breaking of connectivity. PloS one 8: e64339.
15. Jiao QJ, Huang Y, Liu W, Wang XF, Chen XS, et al. (2013) Revealing the hidden relationship by sparse modules in complex networks with a large-scale analysis. PloS one 8: e66020.
16. Baptista MS, Ren HP, Swarts JCM, Carareto R, Nijmeijer H, et al. (2012) Collective almost synchronisation in complex networks. PloS one 7: e48118.
17. Pecora LM, Carroll TL (1998) Master stability functions for synchronized coupled systems. Physical Review Letters 80: 2109–2112.
18. Yang J, Hu G, Xiao J (1998) Chaos synchronization in coupled chaotic oscillators with multiple positive lyapunov exponents. Physical review letters 80: 496–499.
19. Wei G, Zhan M, Lai CH (2002) Tailoring wavelets for chaos control. Physical review letters 89: 284103.
20. Motter AE, Zhou C, Kurths J (2005) Network synchronization, diffusion, and the paradox of heterogeneity. Physical Review E 71: 016116.
21. Zhou C, Motter AE, Kurths J (2006) Universality in the synchronization of weighted random networks. Physical review letters 96: 034101.
22. Chavez M, Hwang DU, Amann A, Hentschel H, Boccaletti S, et al. (2005) Synchronization is enhanced in weighted complex networks. Phys Rev Lett 94: 218701.
23. Wang X, Lai YC, Lai CH (2007) Enhancing synchronization based on complex gradient networks. Physical Review E 75: 056205.
24. Braiman Y, Lindner JF, Ditto WL (1995) Taming spatiotemporal chaos with disorder. Nature 378: 465–467.
25. Brandt SF, Dellen BK, Wessel R (2006) Synchronization from disordered driving forces in arrays of coupled oscillators. Physical review letters 96: 034104.
26. Tessone CJ, Mirasso CR, Toral R, Gunton JD (2006) Diversity-induced resonance. Physical review letters 97: 194101.
27. Brede M (2008) Synchrony-optimized networks of non-identical kuramoto oscillators. Physics Letters A 372: 2618–2622.
28. Wu Y, Xiao J, Hu G, Zhan M (2012) Synchronizing large number of nonidentical oscillators with small coupling. EPL (Europhysics Letters) 97: 40005.
29. Acharyya S, Amritkar RE (2012) Synchronization of coupled nonidentical dynamical systems. EPL (Europhysics Letters) 99: 40005.
30. Goldstein H, Poole CP, Safko JL (2002) Classical Mechanics. New York: Addison-Wesley, 3rd edition.
31. Morin D (2008) Introduction to Classical Mechanics: With Problems and Solutions. Cambridge University Press.
32. Ashcroft NW, Mermin ND (1976) Solid State Physics. Philadelphia: Saunders College.
33. Cui Q, Bahar I (2010) Normal mode analysis: theory and applications to biological and chemical systems. CRC press.
34. Bahar I, Lezon TR, Bakan A, Shrivastava IH (2009) Normal mode analysis of biomolecular structures: functional mechanisms of membrane proteins. Chemical reviews 110: 1463–1497.
35. Kim BJ, Hong H, Choi M (2003) Netons: vibrations of complex networks. Journal of Physics A: Mathematical and General 36: 6329–6336.
36. Estrada E (2010) Universality in protein residue networks. Biophysical journal 98: 890–900.
37. Estrada E, Hatano N, Benzi M (2012) The physics of communicability in complex networks. Physics Reports 514: 89–119.
38. Ren J, Li B (2009) Thermodynamic stability of small-world oscillator networks: A case study of proteins. Physical Review E 79: 051922.
39. Erdős P, Rényi A (1960) On the evolution of random graphs. Publ Math Inst Hungar Acad Sci 5: 17–61.
40. Barabási AL, Albert R (1999) Emergence of scaling in random networks. science 286: 509–512.
41. Watts DJ, Strogatz SH (1998) Collective dynamics of small-worldnetworks. nature 393: 440–442.
42. Chung F, Lu L, Vu V (2003) Spectra of random graphs with given expected degrees. Proceedings of the National Academy of Sciences 100: 6313–6318.
43. Zhan M, Gao J, Wu Y, Xiao J (2007) Chaos synchronization in coupled systems by applying pinning control. Physical Review E 76: 036203.
44. Liu YY, Slotine JJ, Barabási AL (2011) Controllability of complex networks. Nature 473: 167–173.
45. Yan G, Ren J, Lai YC, Lai CH, Li B (2012) Controlling complex networks: How much energy is needed? Physical Review Letters 108: 218703.